# The impacts of mortality rate and strong Allee effect in a three-species food chain model with Crowley–Martin functional response

Siti Nurnabihah Karim[1] Tau Keong Ang[2]
Hamizah Mohd Safuan[3] Sze Qi Chan[4]

(Received 28 January 2025; revised 30 July 2025)

**Abstract**

In ecology, a strong Allee effect is closely associated with population sustainability to extinction. To address this topic, we propose and investigate the intricate features of a three-species food chain model subjected to Crowley–Martin functional response and a strong Allee effect in prey. Here, our focus is to examine how the mortality rate of the middle predator can influence the species interactions. Numerical simulations and stability analysis are utilised to demonstrate the dynamics of the proposed model. The stability analysis is performed using linearization methods on each equilibrium point. Using Sotomayor's theorem, the occurrence of transcritical bifurcations are investigated.

DOI:10.21914/anziamproc.v66.19577, © Austral. Mathematical Soc. 2025. Published 2025-12-08, as part of the Proceedings of the 21st Biennial Computational Techniques and Applications Conference. ISSN 1445-8810. (Print two pages per sheet of paper.) Copies of this article must not be made otherwise available on the internet; instead link directly to the DOI for this article.

Through bifurcation analysis, we observe bi-stability as well as Hopf and transcritical bifurcations. We observe that all species maintain their viability at medium mortality rates, whereas extinction occurs at low mortality rates.

# Contents



# 1 Introduction

Prey-predator interactions are one of the key components of ecological research, offering a basis for understanding the nature of food chains. Numerous ecological frameworks have been constructed to explain these interactions, including the Lotka–Volterra model [7] and the food chain model. Recently, the exploration of three-dimensional food chain models is drawing interest due to their potential to generate complex dynamics in ecosystems [6, 9]. Extensive research has also focused on the Holling Type II functional response due to its half-saturation constants, which are relevant for capturing key biological processes, such as the limiting effects of handling time on predator

consumption rates [16]. This functional response is expressed as

$$\frac{bXY}{\delta + X},$$

where $X$ denotes prey densities, $Y$ denotes predator densities, $b$ represents the predation rate and $\delta$ is the half-saturation constant. A Holling Type II functional response occurs when the rate of prey consumption increases simultaneously with an increase in prey density [2]. Research by Dupke et al. [4] also supports the notion that increased prey density raises the predation rate until it reaches a saturation phase. Distinct from the Holling Type II functional response, is the Crowley–Martin functional response [3]

$$\frac{pXY}{1 + wX + vY + wvXY},$$

where $p$ denotes the feeding rate, $w$ signifies the predator's handling time and $v$ indicates the magnitude of interference among predators. The Crowley–Martin functional response reveals that during prey hunting, predators may hinder one another's endeavors. Research suggests that the predation rate declines as predator density increases, even with high prey density. Research conducted by Sk et al. [15] and Sajan et al. [13] on the Crowley–Martin functional response reveals that systems incorporating this response can exhibit richer dynamics, including bi-stability and tri-stability, which are generally not observed in models using other functional responses.

In most food chain models, prey exhibits logistic growth patterns. However, in real ecosystems, there are events where low-density populations exhibit positive correlation between growth rate and population density, unlike logistic growth. This natural event, referred to as the Allee effect [1], happens when a species participates in mutual hunting or defence against predators. A population influenced by the Allee effect is described by the equation

$$\frac{dX}{d\tau} = rX\left(1 - \frac{X}{K}\right)(X - \gamma),$$

where $r$ denotes the prey's natural growth rate, $K$ is the environmental carrying capacity and $\gamma$ denotes the Allee threshold. According to the equation, the population grows at a rate $r$ and is constrained by the environmental carrying capacity $K$. The growth of the population is concurrently affected by the Allee effect, denoted by the term $(X-\gamma)$. When $0<\gamma<K$, it indicates a strong Allee effect, while $K \leq 0$ indicates a weak Allee effect. Studies reveal that the Allee effect, especially the strong one, can lead to either species survival or extinction [6, 14].

Real-world instances pertinent to ecological modelling include the interaction between mosquitoes and the water bug predator in freshwater wetlands, which follows the Crowley–Martin functional response [8], as well as Atlantic cod (*Gadus morhua*) that exhibit the Allee effect [11]. Both the studies unveil interesting dynamics that motivate the current article. This study addresses the integration of the Crowley–Martin functional response with a strong Allee effect in analysing the dynamics of food chain models and generates new insights in understanding species behaviour.

A study by Saha and Samanta [12] highlighted that the mortality rate is crucial in regulating system dynamics. On the other hand, Ye et al. [17] revealed that in the presence of the Allee effect, increased predator mortality enhances prey productivity and reduces rivalry among predators for prey. Taking a similar approach, we focus on mortality rates as the bifurcation parameter in this study; however, we include the influence of a strong Allee effect in species interaction. Inspired by previous ecological discoveries, this article examines how alterations in mortality rates can disturb the stability of food chain models. We are also interested in how a strong Allee effect in prey affects the species interactions. By analysing the variations in mortality rates, we recognise dynamical patterns that may serve as indicators in natural environments.

# 2 Food chain model

This study evaluates a prey-predator model simulating the food chain model of prey $X$, middle predator $Y$ and top predator $Z$, as proposed by Hastings and Powell [5]. Our model integrates a Holling Type II functional response between $X$ and $Y$ with a Crowley–Martin functional response between $Y$ and $Z$ while considering a strong Allee effect on $X$:

$$\begin{aligned}
\frac{dX}{d\tau} &= rX\left(1-\frac{X}{K}\right)(X-\gamma)-\frac{bXY}{\delta+X},\\
\frac{dY}{d\tau} &= \frac{nXY}{\delta+X}-\frac{pYZ}{1+wY+\nu Z+w\nu YZ}-qY,\\
\frac{dZ}{d\tau} &= \frac{sYZ}{1+wY+\nu Z+w\nu YZ}-cZ,
\end{aligned} \tag{1}$$

where $n$ is a conversion rate from prey to middle predator, $q$ is the middle predator's natural death rate, $s$ is the middle predator's conversion rate to top predator, and $c$ is the top predator's natural death rate.

Non-dimensionalization is applied to model (1) to decrease the amount of variables utilizing the scaled parameters:

$$t = rK\tau, \quad x=\frac{X}{K}, \quad y=\frac{bY}{rK^2} \quad \text{and} \quad z=\frac{pZ}{rK}.$$

Then, we obtain the non-dimensional model

$$\begin{aligned}
\frac{dx}{dt} &= x(1-x)(x-\eta)-\frac{xy}{\mu+x},\\
\frac{dy}{dt} &= \frac{\sigma_1 xy}{\mu+x}-\frac{yz}{m_3yz+m_1y+m_2z+1}-\rho_1 y,\\
\frac{dz}{dt} &= \frac{\sigma_2 yz}{m_3yz+m_1y+m_2z+1}-\rho_2 z,
\end{aligned} \tag{2}$$

where $\eta=\gamma/K$, $\mu=\delta/K$, $\sigma_1=n/rK$, $m_1=wrK^2/b$, $m_2=\nu rK/p$, $m_3=w\nu r^2K^3/(bp)$, $\rho_1=q/(rK)$, $\sigma_2=sK/b$ and $\rho_2=c/(rK)$.

Table 1: Stability analysis of model (2).

| Equilibrium point | Stability conditions |
|---|---|
| $P_0(0,0,0)$ | Always stable |
| $P_1(1,0,0)$ | $\rho_1 > \sigma_1/(\mu+1)$ and $\eta < 1$ |
| $P_2(x_2,0,0)$ | $\eta > 1$ and $\rho_1 > \eta\sigma_1/(\mu+\eta)$ |
| $P_3(x_3,y_3,0)$ | $\rho_2(1+m_1y_3) > \sigma_2y_3$ and $\mu y_3 > (\mu+x_3)^2\,[(x_3-\eta)(1-x_3)+x_3(1+\eta-2x_3)]$ |
| $P_4(x_4,y_4,z_4)$ | $D_1 > 0$, $D_1D_2 - D_3 > 0$ and $D_3 > 0$ |

There are five distinct equilibrium points exhibited by model (2) (the expressions for $x_i$, $y_i$ and $z_i$, with $i = 2,3,4$, are listed in Appendix A):

1. extinction equilibrium, $P_0(0,0,0)$;
2. axial equilibriums, $P_1(1,0,0)$ and $P_2(x_2,0,0)$;
3. top predator-free equilibrium, $P_3(x_3,y_3,0)$; and
4. coexistence equilibrium, $P_4(x_4,y_4,z_4)$.

The Jacobian matrix associated with model (2) is

$$J(x,y,z) = \begin{bmatrix} J_{11} & J_{12} & 0 \\ J_{21} & J_{22} & J_{23} \\ 0 & J_{32} & J_{33} \end{bmatrix}, \tag{3}$$

where $J_{ij}$, with $i,j = 1,2,3$, are listed in Appendix B. Utilizing Jacobian matrix (3), we conduct a stability analysis using the linearization approach at each equilibrium point, and apply the Routh–Hurwitz criterion at the coexistence equilibrium point, as listed in Table 1. The proof of this analysis is given in Appendix C.

Additionally, we examine the occurrence of bifurcations in model (2) with respect to the middle predator's mortality rate $\rho_1$. The conditions for transcritical bifurcation (TB) are derived through Sotomayor's theorem [10].

**Theorem 1.** *(1) A transcritical bifurcation, named* $TB_2$*, arises from* $P_1$ *at*

$$\rho_1 = \rho_1^{TB_2} = \frac{\sigma_1}{\mu+1}.$$

*(2) A transcritical bifurcation, named* $TB_1$*, arises from* $P_3$ *at*

$$\rho_1 = \rho_1^{TB_1} = \frac{\sigma_1(\sigma_2-\rho_2 m_1)(\hat{x}-\eta)(\mu+\hat{x})-\rho_2\sigma_1}{(1+\mu)(\sigma_2-\rho_2 m_1)(\hat{x}-\eta)(\mu+\hat{x})-\rho_2}.$$

**Proof:** For case (1), the Jacobian matrix $J(P_1)=0$ possesses a zero eigenvalue when $\rho_1=\rho_1^{TB_2}=\sigma_1/(\mu+1)$. The eigenvectors associated with the zero eigenvalues of $J(P_1)$ and $J(P_1)^T$, respectively, are

$$v=\begin{bmatrix}\frac{1}{(\mu+1)(\eta-1)}\\ 1\\ 0\end{bmatrix};\quad w=\begin{bmatrix}0\\1\\0\end{bmatrix}.$$

Let

$$f=\begin{bmatrix}f_1\\f_2\\f_3\end{bmatrix}=\begin{bmatrix}x(1-x)(x-\eta)-\frac{xy}{\mu+x}\\ \frac{\sigma_1 xy}{\mu+x}-\frac{yz}{m_3yz+m_1y+m_2z+1}-\rho_1 y\\ \frac{\sigma_2 yz}{m_3yz+m_1y+m_2z+1}-\rho_2 z\end{bmatrix}.$$

Then, we employ Sotomayor's theorem [10] to evaluate the conditions of

(TB1) $w^T f_{\rho_1}(P_1;\rho_1^{TB_2})=\begin{bmatrix}0&1&0\end{bmatrix}\cdot\begin{bmatrix}0\\0\\0\end{bmatrix}=0,$

(TB2) $w^T[Df_{\rho_1}(P_1;\rho_1^{TB_2})v]=\begin{bmatrix}0&1&0\end{bmatrix}\cdot\begin{bmatrix}0\\-1\\0\end{bmatrix}=-1\neq 0,$

(TB3) $w^T[D^2f(P_1;\rho_1^{TB_2})(v,v)]=\begin{bmatrix}0&1&0\end{bmatrix}\cdot\begin{bmatrix}\frac{2\eta-2\mu-4}{(\eta-1)^2(\mu+1)^3}\\ \frac{2\sigma_1\mu}{(\mu+1)^3(\eta-1)}\\0\end{bmatrix}=\frac{2\sigma_1\mu}{(\mu+1)^3(\eta-1)}\neq 0.$

Consequently, we conclude that at $P_1$, a transcritical bifurcation is exhibited by model (2) as $\rho_1$ surpasses $\rho_1^{TB_2} = \frac{\sigma_1}{\mu+1}$ since the criteria (TB1)–(TB3) are satisfied.

The proof for case (2) is similar and therefore it is omitted. ♠

# 3 Results and discussion

In order to analyse the dynamics of model (2), a bifurcation analysis is conducted by varying the mortality rate of middle predator $\rho_1$. The bifurcation plots are acquired using MatCont with parameter values of $\eta = 0.12$, $\mu = 0.81$, $\sigma_1 = 4.88$, $\sigma_2 = 2.22$, $m_1 = 0.51$, $m_2 = 0.19$, $m_3 = 1.15$ and $\rho_2 = 0.13$.

For prey, middle predator and top predator, respectively, Figures 1, 2 and 3 illustrate model (2) as $\rho_1$ varies. The stable steady states are shown as blue solid curves, the unstable steady states as red dotted curves, and green dotted lines to delineate different regions, I, II, III, IV and V. Labels in these plots are: H (Hopf bifurcation); TB (transcritical bifurcation); and LPC (limit point of cycles). Model (2) exhibits transcritical bifurcations at $TB_1$ ($\rho_1 = 2.646$) and $TB_2$ ($\rho_1 = 2.696$), and a Hopf bifurcation at H ($\rho_1 = 1.75$). These bifurcations divide the diagrams into the five distinct regions (I, II, III, IV and V). For each region, we set a specific value (Table 2) and generate phase portraits with time series diagrams to study the underlying patterns of the populations over time.

According to Figures 1, 2 and 3, in Region I (low $\rho_1$; $\rho_1$ between 0 and 1.49), $P_0$ is stable (Figure 4) as a low mortality rate indicates a slightly high middle predator population which poses a threat for prey. Additionally, a strong Allee effect also hampers prey growth; over time, both middle and top predators get insufficient food for survival, leading to their extinction.

Meanwhile, Region II (medium-low $\rho_1$; $\rho_1$ between 1.49 and 1.75) highlights

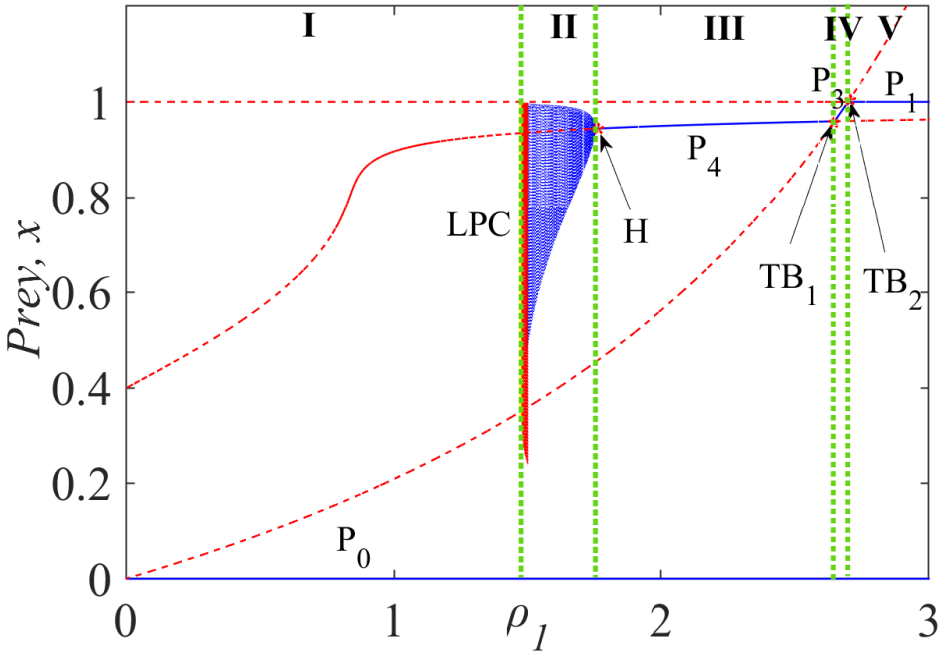


Figure 1: Bifurcation plot of model (2) corresponding to $\rho_1$ for each species of prey.

the presence of a supercritical Hopf bifurcation on $P_4$. Oscillatory behaviour is observed, as depicted in Figure 5(a), where the densities of all three species fluctuate over time, consequently disrupting their coexistence. Simultaneously, we see that $P_0$ is also stable (Figure 5(b)), clarifying an instance of bi-stability. Depending on the initial value, the species typically attain one of the steady states, as illustrated in Figure 5(c).

In Region III (moderate $\rho_1$; $\rho_1$ between 1.75 and 2.646), the bi-stability persists between $P_4$ and $P_0$, reliant on the initial value. At a high initial value (Figure 6(a)), cohabitation occurs since the medium mortality rate contributes to the ideal density of the middle predator, hence enhancing the

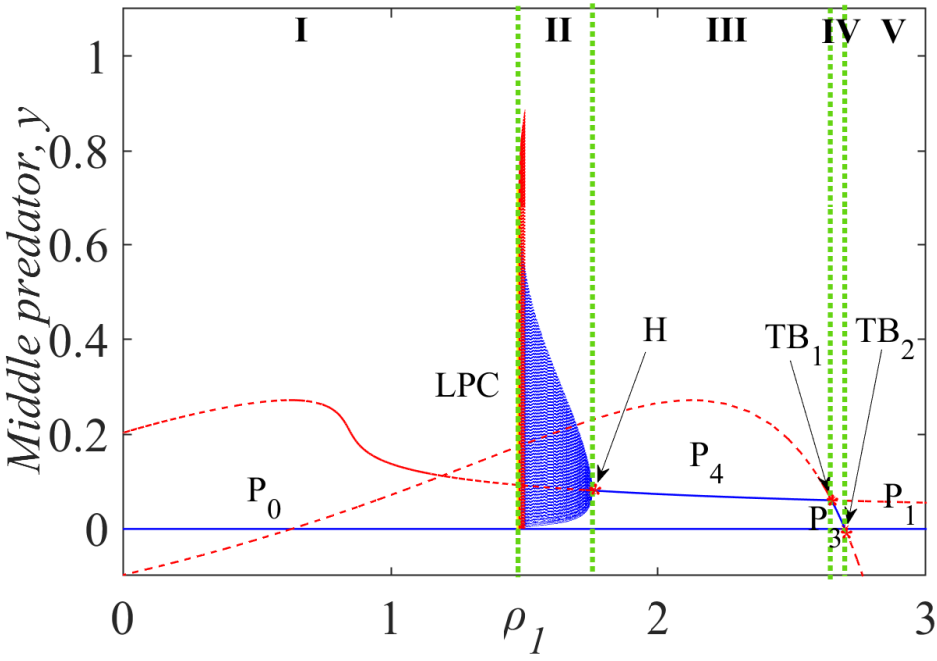


Figure 2: Bifurcation plot of model (2) corresponding to $\rho_1$ for each species of middle predator.

survival of the top predator. At the same time, a strong Allee effect assists the proliferation of prey. Conversely, populations that initiate with low density (Figure 6(b)) are vulnerable to extinction due to hunting pressures.

Furthermore, in Region IV (medium-high $\rho_1$; $\rho_1$ between 2.646 and 2.696), $P_3$ is stable (Figure 7(a)). This is because middle predator densities gradually decrease over time due to the comparatively high mortality rate, making them unfavourable for the sustenance of the top predator. Moreover, extinction of all species occurs at a lower initial value, reflected by the bi-stability (Figure 7(b)).

Region V (high $\rho_1$; $\rho_1$ is greater than 2.696) may pose a threat to the longevity

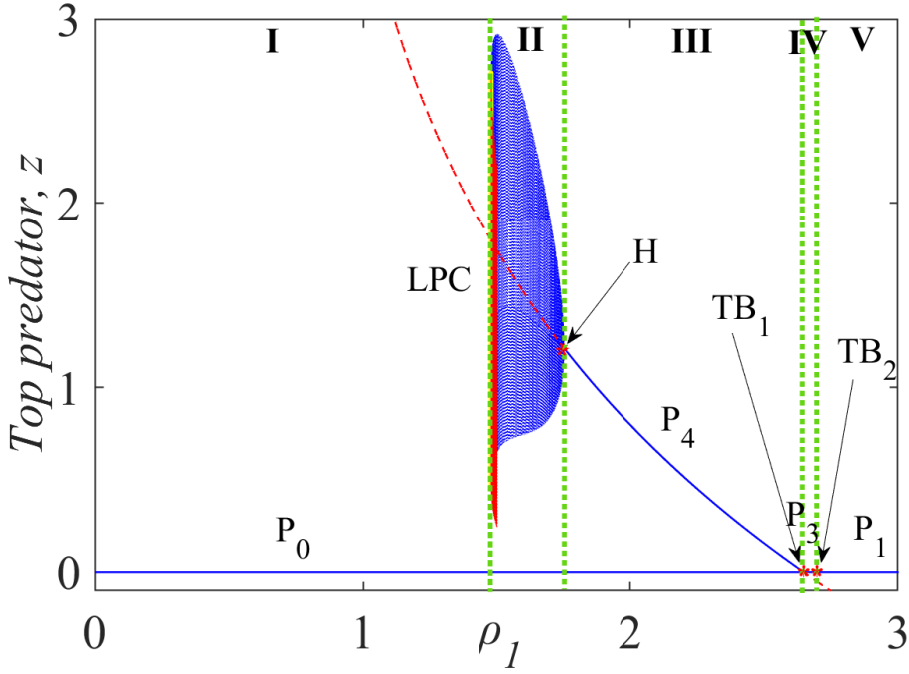


Figure 3: Bifurcation plot of model (2) corresponding to $\rho_1$ for each species of top predator.

of both the middle and top predators, as $P_1$ is now stable (Figure 8(a)). The extinction of the middle predator is facilitated by the high mortality rate, which they are incapable of overcomming and only prey survives due to the influence of a strong Allee effect. Likewise, $P_0$ is stable, indicating the bi-stability.

Region II is the ideal region for ensuring the sustainability of the population. The medium-low mortality rate suggests the natural circumstances are conducive to long-term population stability. Additionally, Region I with low $\rho_1$ is unfavorable to the population and should be avoided.

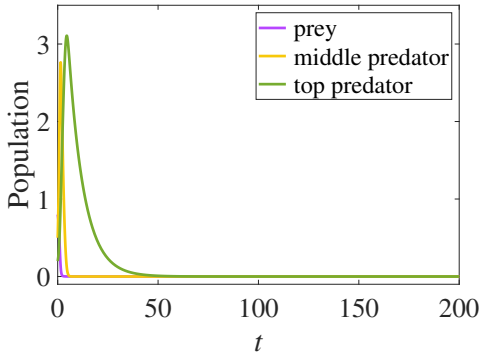


(a)

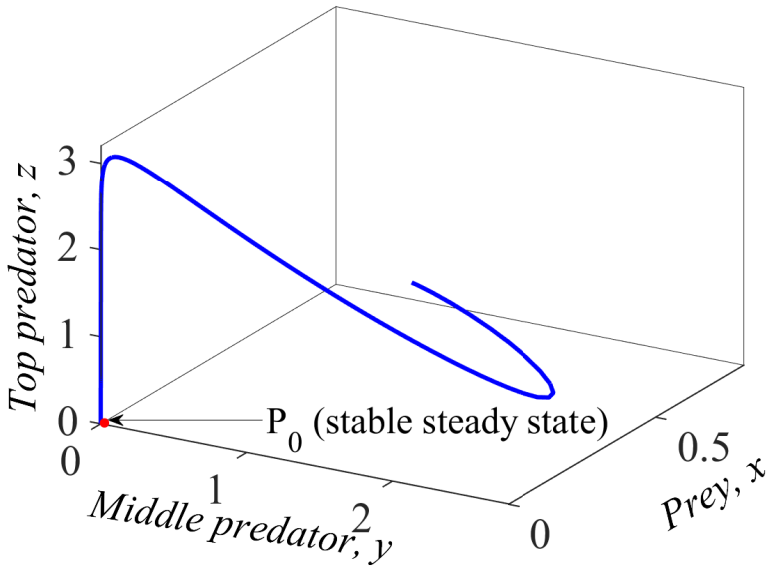


(b)

Figure 4: Time series diagrams at $\rho_1 = 0.5$ with initial value (a) $(0.8, 0.5, 0.2)$ and (b) the phase portrait.

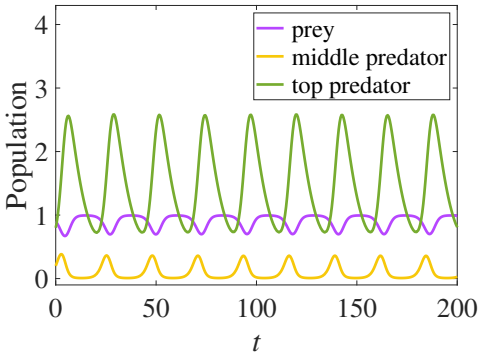


(a)

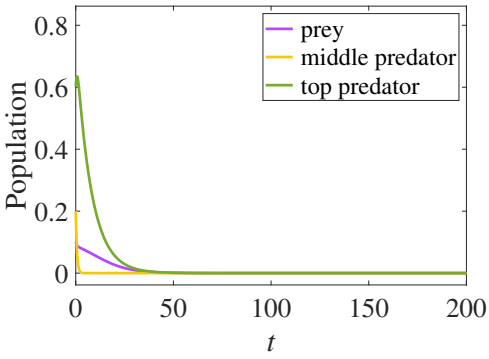


(b)

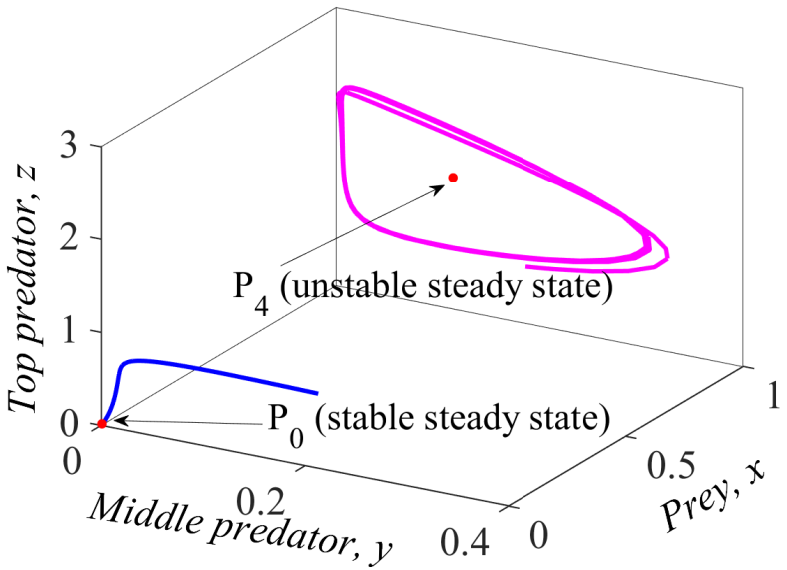


(c)

Figure 5: Time series diagrams at $\rho_1 = 1.6$ with initial values (a) $(0.9, 0.4, 0.8)$ and (b) $(0.1, 0.2, 0.6)$, and (c) the phase portrait.

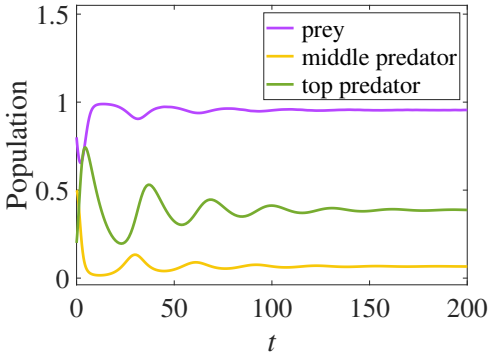


(a)

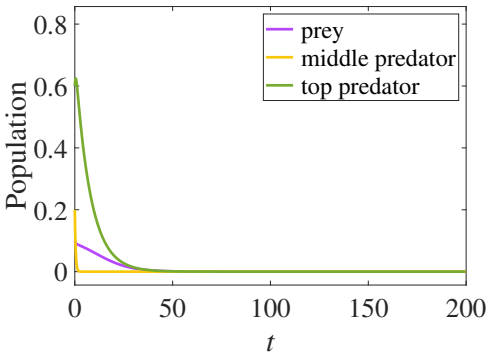


(b)

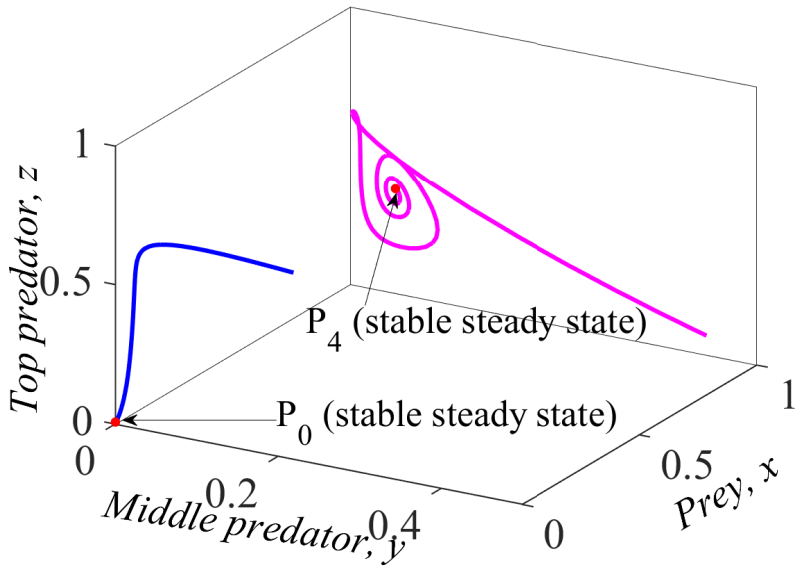


(c)

Figure 6: Time series diagrams at $\rho_1 = 2.3$ with initial values (a) $(0.8, 0.5, 0.7)$ and (b) $(0.1, 0.2, 0.6)$, and (c) the phase portrait.

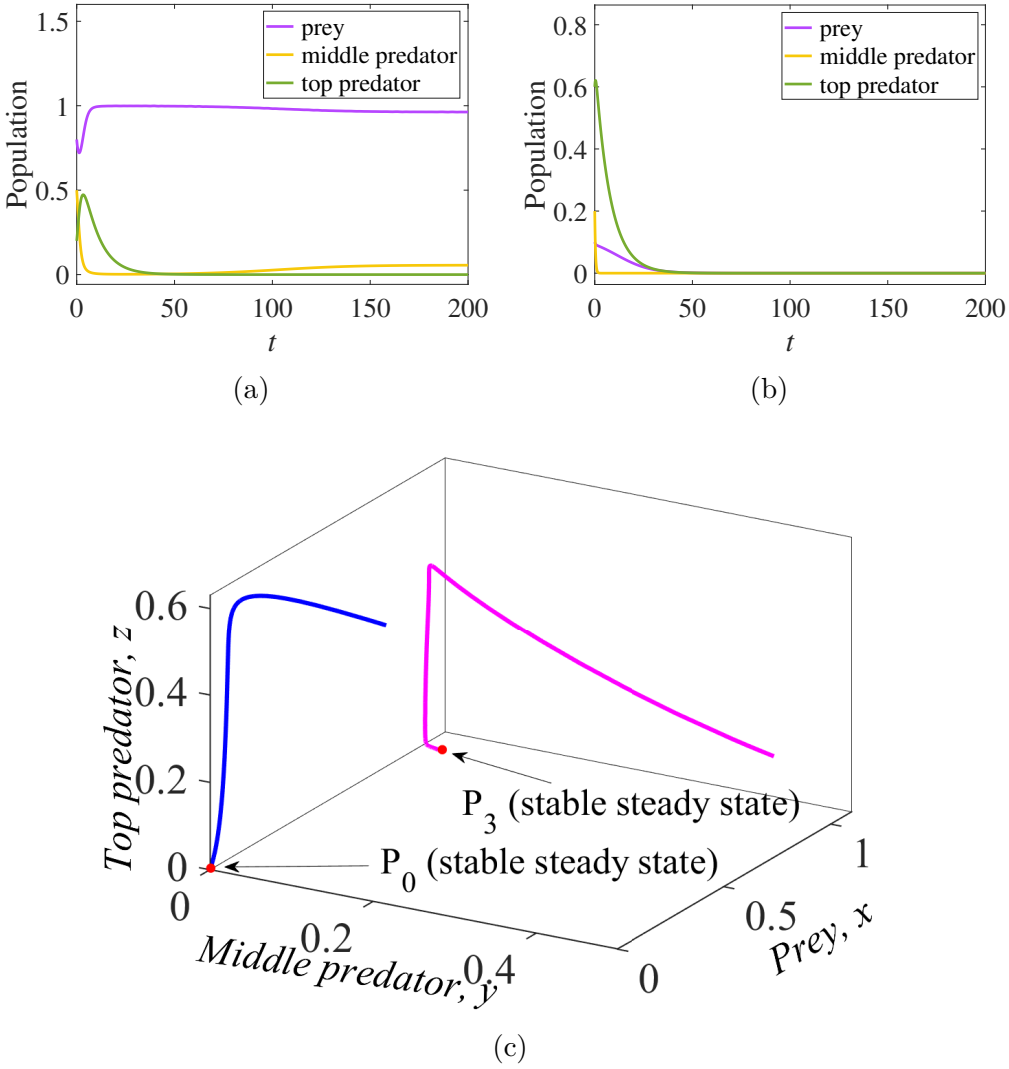


Figure 7: Time series diagrams at $\rho_1 = 2.65$ with initial values (a) $(0.8, 0.4, 0.7)$ and (b) $(0.1, 0.2, 0.6)$, and (c) the phase portrait.

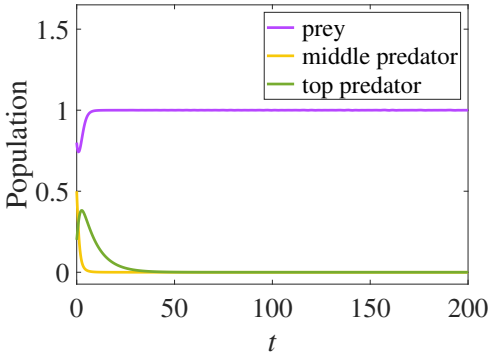


(a)

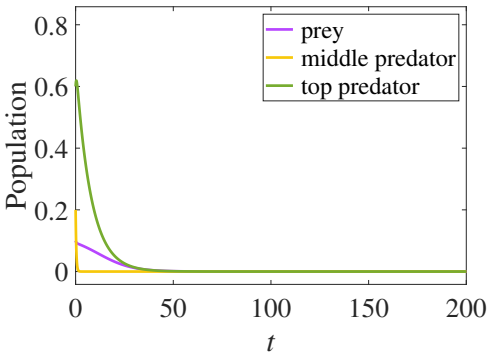


(b)

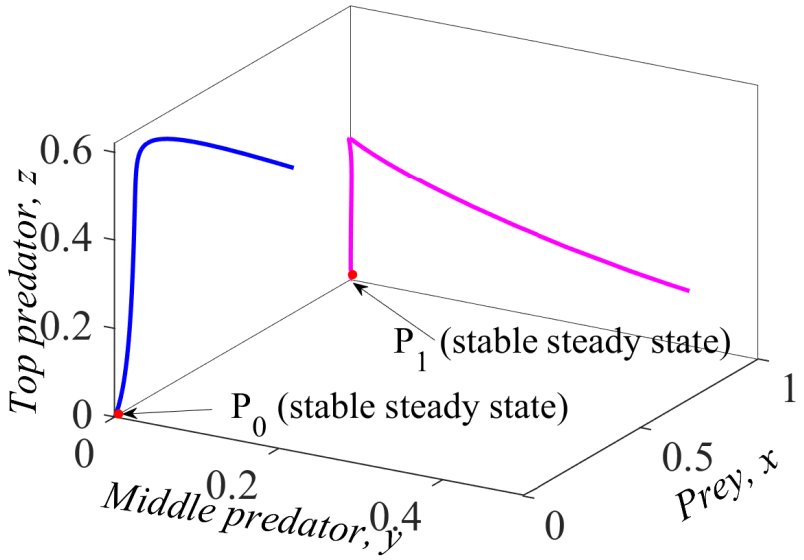


(c)

Figure 8: Time series diagrams at $\rho_1 = 2.9$ with initial values (a) $(0.8, 0.4, 0.7)$ and (b) $(0.1, 0.2, 0.6)$, with (c) the phase portrait.

Table 2: Numerical results of model (2).

| $\rho_1$ | Steady state | Eigenvalues | Property | Figure |
|---|---|---|---|---|
| 0.5 | $(0, 0, 0)$ | $-0.12, -0.5, -0.13$ | Stable | 4(a) |
| 1.6 | $(0.94, 0.09, 1.51)$ | $-0.62, 0.01 \pm 0.3i$ | Unstable | 5(a) |
| | $(0, 0, 0)$ | $-0.12, -1.6, -0.13$ | Stable | 5(b) |
| 2.3 | $(0.95, 0.07, 0.39)$ | $-0.67, -0.03 \pm 0.2i$ | Stable | 6(a) |
| | $(0, 0, 0)$ | $-0.12, -2.3, -0.13$ | Stable | 6(b) |
| 2.65 | $(0.96, 0.06, 0)$ | $-0.01, -0.05, -0.7$ | Stable | 7(a) |
| | $(0, 0, 0)$ | $-0.12, -2.65, -0.13$ | Stable | 7(b) |
| 2.9 | $(1, 0, 0)$ | $-0.88, -0.2, -0.13$ | Stable | 8(a) |
| | $(0, 0, 0)$ | $-0.12, -2.9, -0.13$ | Stable | 8(b) |

# 4 Conclusion

This study analyses a three-species food chain model, considering the influence of a strong Allee effect with a Crowley–Martin functional response. This model seeks to comprehend the intricate species interactions in the context of food chains. The stability of equilibrium points is assessed using the linearization approach and the Routh–Hurwitz criterion. The role of the mortality rate of the middle predator has been explored via the bifurcation diagrams, phase portraits and time series across various mortality rate values. The medium mortality rate of the middle predator is vital as it impacts the stability of the coexistence steady state. The findings indicate a connection between variations in the middle predator's mortality rate and shifts in population densities. An increase in the middle predator's mortality rate may reduce the top predator population. In this scenario, the presence of a strong Allee effect on prey enhances their survivability. Therefore, to preserve a balanced ecosystem, it is imperative to establish a proper strategy to maintain the optimal mortality rate. Further research into the model's dynamical behaviours, incorporating other ecological factors like herd and fear refuge, would be intriguing and deserve further consideration.

## 4.1 Acknowledgements

Authors acknowledge the Ministry of Higher Education Malaysia and Research Management Centre-UTM, Universiti Teknologi Malaysia for financial assistance under UTM Encouragement Research (UTMER) with vote number Q.J130000.3854.31J08. Moreover, authors thank the support provided by the UoSM Seed Fund (UoSM/SF2023/09) from the University of Southampton Malaysia awarded to Sze Qi Chan.

# A Expressions of $x_i$, $y_i$ and $z_i$

The expressions $x_i$, $y_i$ and $z_i$ $(i = 2, 3, 4)$ are:

$$
\begin{aligned}
x_2 &= \eta\,,\\
x_3 &= \frac{\mu\rho_1}{\sigma_1 - \rho_1}\,,\\
y_3 &= (1 - x_3)(x_3 - \eta)(\mu + x_3)\,,\\
&\text{$x_4$ is the positive root of:}\\
&\quad A_0x^6 + A_1x^5 + A_2x^4 + A_3x^3 + A_4x^2 + A_5x + A_6 = 0\,,\ \text{where}\\
A_0 &= \sigma_1\sigma_2m_3 - \sigma_2m_3\rho_1\,,\\
A_1 &= \sigma_2m_3[\sigma_1(\mu - 2\eta - 2) + 2\rho_1(\eta - \mu + 1)]\,,\\
A_2 &= \sigma_2m_3\Big(\rho_1[4\mu + \eta(4\mu - 4) - \eta^2 - \mu^2 - 1]\\
&\qquad +\sigma_1[\eta^2 + \eta(4 - 2\mu) - 2\mu + 1]\Big)\,,\\
A_3 &= \sigma_2\Big[m_3\Big(\eta^2[\rho_1(2 - 2\mu) + \sigma_1(\mu - 2)]\\
&\qquad +\eta[\rho_1(2\mu^2 - 8\mu + 2) + 4\mu\sigma_1 - 2\sigma_1]\\
&\qquad +\mu[2\rho_1(\mu - 1) + \sigma_1]\Big) + m_2\rho_1 - m_2\sigma_1 + 1\Big] - m_1\rho_2\,,\\
A_4 &= \sigma_2\Big(\eta^2m_3[\sigma_1 - \mu^2\rho_1 + \mu(4\rho_1 - 2\sigma_1) - \rho_1]\\
&\qquad +\eta[m_2\sigma_1 - 4\mu^2m_3\rho_1 + 2\mu m_3(2\rho_1 - \sigma_1) - m_2\rho_1 - 1]\\
&\qquad -\mu^2m_3\rho_1 + \mu(m_2\rho_1 + 1) - m_2\rho_1 + m_2\sigma_1 - 1\Big) + \rho_2m_1(\eta - \mu + 1)\,,
\end{aligned}
$$

$$
\begin{aligned}
A_5 &= \sigma_2 \Big( m_3 \mu \eta^2 (2\mu\rho_1 - 2\rho_1 + \sigma_1) \\
&\quad + \eta [2\mu^2 m_3 \rho_1 - \mu(m_2\rho_1 + 1) + m_2\rho_1 - m_2\sigma_1 + 1] \\
&\quad - \mu(m_2\rho_1 + 1) \Big) + \rho_2 m_1 [\eta(\mu - 1) + \mu] \,, \\
A_6 &= \eta\mu(\sigma_2 m_2 \rho_1 - m_1\rho_2 + \sigma_2) - \eta^2\mu^2\sigma_2 m_3\rho_1 + \rho_2 \,, \\
y_4 &= (1 - x_4)(x_4 - \eta)(\mu + x_4) \,, \\
z_4 &= \frac{(1 - x_4)(x_4 - \eta)(\mu + x_4)(\sigma_2 - \rho_2 m_1) - \rho_2}{\rho_2 (m_3(1 - x_4)(x_4 - \eta)(\mu + x_4) + m_2)} \,.
\end{aligned}
$$

# B Expressions of $J_{ij}$

The expressions $J_{ij}$ $(i, j = 1, 2, 3)$ are:

$$
\begin{aligned}
J_{11} &= (x - \eta)(1 - x) + x(1 - 2x + \eta) - \frac{y\mu}{(\mu + x)^2} \,, \\
J_{12} &= -\frac{x}{\mu + x} \,, \\
J_{21} &= \frac{\sigma_1 y \mu}{(\mu + x)^2} \,, \\
J_{22} &= \frac{\sigma_1 x}{\mu + x} - \frac{z(m_2 z + 1)}{(m_3 y z + m_1 y + m_2 z + 1)^2} - \rho_1 \,, \\
J_{23} &= -\frac{y(m_1 y + 1)}{(m_3 y z + m_1 y + m_2 z + 1)^2} \,, \\
J_{32} &= \frac{\sigma_2 z(m_2 z + 1)}{(m_3 y z + m_1 y + m_2 z + 1)^2} \,, \\
J_{33} &= \frac{\sigma_2 y(m_1 y + 1)}{(m_3 y z + m_1 y + m_2 z + 1)^2} - \rho_2 \,.
\end{aligned}
$$

# C Proof of Stability Analysis

### Stability of extinction equilibrium, $P_0$

The Jacobian matrix at $P_0$ is

$$J(P_0) = \begin{bmatrix} -\eta & 0 & 0 \\ 0 & -\rho_1 & 0 \\ 0 & 0 & -\rho_2 \end{bmatrix}.$$

The eigenvalues of $J(P_0)$ are $-\eta$, $-\rho_1$ and $-\rho_2$ which are negative values. This indicates that $P_0$ is always stable.

### Stability of axial equilibrium, $P_1$

The Jacobian matrix at $P_1$ is

$$J(P_1) = \begin{bmatrix} \eta - 1 & -\frac{1}{\mu+1} & 0 \\ 0 & \frac{\sigma_1}{\mu+1} - \rho_1 & 0 \\ 0 & 0 & -\rho_2 \end{bmatrix}.$$

The eigenvalues of $J(P_1)$ are $\eta - 1$, $\sigma_1/(\mu+1) - \rho_1$ and $-\rho_2$. This indicates that $P_1$ is stable when $\rho_1 > \sigma_1/(\mu+1)$ and $\eta < 1$.

### Stability of axial equilibrium, $P_2$

The Jacobian matrix at $P_2$ is

$$J(P_2) = \begin{bmatrix} -\eta^2 + \eta & -\frac{\eta}{\mu+\eta} & 0 \\ 0 & \frac{\eta\sigma_1}{\mu+\eta} - \rho_1 & 0 \\ 0 & 0 & -\rho_2 \end{bmatrix}.$$

The eigenvalues of $J(P_2)$ are $-\eta^2+\eta$, $\eta\sigma_1/(\mu+\eta)-\rho_1$ and $-\rho_2$. This indicates that $P_2$ is stable when $\eta > 1$ and $\rho_1 > \eta\sigma_1/(\mu+\eta)$.

### Stability of top predator-free equilibrium, $P_3$

The Jacobian matrix at $P_3$ is

$$J(P_3) = \begin{bmatrix} 1 - x_3(x_3 - \eta) + x_3(1 + \eta - 2x_3) - \frac{\mu y_3}{(\mu + x_3)^2} & -\frac{x_3}{\mu + x_3} & 0 \\ \frac{\sigma_1 \mu y_3}{(\mu + x_3)^2} & 0 & -\frac{y_3}{m_1 y_3 + 1} \\ 0 & 0 & \frac{\sigma_2 y_3}{m_1 y_3 + 1} - \rho_2 \end{bmatrix}.$$

One eigenvalue of $J(P_3)$ is $\sigma_2 y_3/(m_1 y_3 + 1) - \rho_2$ and the other two eigenvalues are obtained from the matrix

$$\begin{bmatrix} 1 - x_3(x_3 - \eta) + x_3(1 + \eta - 2x_3) - \frac{\mu y_3}{(\mu + x_3)^2} & -\frac{x_3}{\mu + x_3} \\ \frac{\sigma_1 \mu y_3}{(\mu + x_3)^2} & 0 \end{bmatrix},$$

with the characteristic polynomial

$$\lambda^2 - \frac{(\mu + x_3)^2[(1 - x_3)(x_3 - \eta) + x_3(1 + \eta - 2x_3)] - \mu y_3}{(\mu + x_3)^2}\lambda + \frac{\sigma_1 \mu x_3 y_3}{(\mu + x_3)^3}.$$

This signifies that $P_3$ is stable when $\rho_2(1 + m_1 y_3) > \sigma_2 y_3$ and $\mu y_3 > (\mu + x_3)^2[(x_3 - \eta)(1 - x_3) + x_3(1 + \eta - 2x_3)]$.

### Stability of coexistence equilibrium, $P_4$

The Jacobian matrix at $P_4$ is

$$J(P_4) = \begin{bmatrix} a_{11} & a_{12} & 0 \\ a_{21} & a_{22} & a_{23} \\ 0 & a_{32} & a_{33} \end{bmatrix},$$

with

$$a_{11} = (x_4 - \eta)(1 - x_4) + x_4(1 - 2x_4 + \eta) - \frac{y_4 \mu}{(\mu + x_4)^2},$$

$$a_{12} = -\frac{x_4}{\mu + x_4},$$

$$
\begin{aligned}
a_{21} &= \frac{\sigma_1 x_4 \mu}{(\mu + x_4)^2}\,, \\
a_{22} &= \frac{\sigma_1 x_4}{\mu + x_4} - \frac{z_4(m_2 z_4 + 1)}{(m_3 y_4 z_4 + m_1 y_4 + m_2 z_4 + 1)^2} - \rho_1\,, \\
a_{23} &= -\frac{y_4(m_1 y_4 + 1)}{(m_3 y_4 z_4 + m_1 y_4 + m_2 z_4 + 1)^2}\,, \\
a_{32} &= \frac{\sigma_2 z_4(m_2 z_4 + 1)}{(m_3 y_4 z_4 + m_1 y_4 + m_2 z_4 + 1)^2}\,, \\
a_{33} &= \frac{\sigma_2 y_4(m_1 y_4 + 1)}{(m_3 y_4 z_4 + m_1 y_4 + m_2 z_4 + 1)^2} - \rho_2\,.
\end{aligned}
$$

From $J(P_4)$, we get the characteristic equation

$$\lambda^3 + D_1\lambda^2 + D_2\lambda + D_3 = 0\,,$$

where

$$
\begin{aligned}
D_1 &= -(a_{11} + a_{22} + a_{33})\,, \\
D_2 &= a_{11}a_{22} + a_{11}a_{33} + a_{22}a_{33} - a_{12}a_{21} - a_{23}a_{32}\,, \\
D_3 &= a_{12}a_{21}a_{33} + a_{11}a_{23}a_{32} - a_{11}a_{22}a_{33}\,.
\end{aligned}
$$

Then, by the Routh–Hurwitz criterion, $P_4$ is stable when $D_1 > 0$, $D_1D_2 - D_3 > 0$ and $D_3 > 0$.

# References


[1] W. C. Allee. "Co-operation among animals". In: *Am. J. Sociol.* 37.3 (1931), pp. 386–398. DOI: 10.1086/215731 (cit. on p. C22).

[2] S. Anshu and B. Dubey. "Bifurcation analysis and spatiotemporal dynamics in a diffusive predator-prey system incorporating a Holling Type II functional response". In: *Int. J. Bifurcat. Chaos* 34.8, 2450105 (2024). DOI: 10.1142/S0218127424501050 (cit. on p. C22).

[3] P. H. Crowley and E. K. Martin. “Functional responses and interference within and between year classes of a dragonfly population”. In: *J. N. Am. Benthol. Soc.* 8.3 (1989), pp. 211–221. DOI: 10.2307/1467324 (cit. on p. C22).

[4] C. Dupke, A. Peters, N. Morellet, and M. Heurich. “Holling meets habitat selection: Functional response of large herbivores revisited”. In: *Movement Ecol.* 9.1, 45 (2021). DOI: 10.1186/s40462-021-00282-6 (cit. on p. C22).

[5] A. Hastings and T. Powell. “Chaos in a three-species food chain”. In: *Ecology* 72.3 (1991), pp. 896–903. DOI: 10.2307/1940591 (cit. on p. C24).

[6] S. N. Karim and T. K. Ang. “Co-dimension 2 bifurcation analysis of a tri-trophic food chain model with strong Allee effect and Crowley–Martin functional response”. In: *Chaos Soliton. Fract.* 186, 115316 (2024). DOI: 10.1016/j.chaos.2024.115316 (cit. on pp. C21, C23).

[7] A. J. Lotka. “Undamped oscillations derived from the law of mass action”. In: *J. Am. Chem. Soc.* 42.8 (1920), pp. 1595–1599. DOI: 10.1021/ja01453a010 (cit. on p. C21).

[8] C. Mukherjee, K. P. Das, and G. Panigrahi. “Dynamics of insect predator and mosquito prey system with mutual interference as a factor for the co-occurrence: Validating through models”. In: *J. Appl. Math.* 1.3, 246 (2023). DOI: 10.59400/jam.v1i3.246 (cit. on p. C23).

[9] S. Pal, P. K. Tiwari, A. K. Misra, and H. Wang. “Fear effect in a three-species food chain model with generalist predator”. In: *Math. Biosci. Eng.* 21.1 (2023), pp. 1–33. DOI: 10.3934/mbe.2024001 (cit. on p. C21).

[10] L. Perko. *Differential Equations and Dynamical Systems*. Texts in Applied Mathematics. Springer New York, 2008. DOI: 10.1007/978-1-4613-0003-8 (cit. on pp. C25, C26).

[11] T. Perälä, J. A. Hutchings, and A. Kuparinen. "Allee effects and the Allee-effect zone in northwest Atlantic cod". In: *Biol. Lett.* 18, 20210439 (2022). DOI: 10.1098/rsbl.2021.0439 (cit. on p. C23).

[12] S. Saha and G. Samanta. "Modelling of a two prey and one predator system with switching effect". In: *Comput. Math. Biophys.* 9.1 (2021), pp. 90–113. DOI: 10.1515/cmb-2020-0120 (cit. on p. C23).

[13] Sajan, A. Kumar, and B. Dubey. "Stability switching in a cooperative prey-predator model with transcritical and Hopf-bifurcations". In: *Nonlinear Dynamics and Applications, Springer Proceedings in Complexity*. Ed. by S. Banerjee and A. Saha. 2022, pp. 987–1000. DOI: 10.1007/978-3-030-99792-2_84 (cit. on p. C22).

[14] B. P. Sarangi and S. N. Raw. "Dynamics of a spatially explicit eco-epidemic model with double Allee effect". In: *Math. Comput. Sim.* 206 (2023), pp. 241–263. DOI: 10.1016/j.matcom.2022.11.004 (cit. on p. C23).

[15] N. Sk, B. Mondal, A. A. Thirthar, M. A. Alqudah, and T. Abdeljawad. "Bistability and tristability in a deterministic prey-predator model: Transitions and emergent patterns in its stochastic counterpart". In: *Chaos Soliton. Fract.* 176 (2023), p. 114073. DOI: 10.1016/j.chaos.2023.114073 (cit. on p. C22).

[16] B. E. Smith and L. A. Smith. "Multispecies functional responses reveal reduced predation at high prey densities and varied responses among and within trophic groups". In: *Fish Fish.* 21.5 (2020), pp. 891–905. DOI: 10.1111/faf.12468 (cit. on p. C22).

[17] J. Ye, Y. Wang, Z. Jin, C. Dai, and M. Zhao. "Dynamics of a predator-prey model with strong Allee effect and nonconstant mortality rate". In: *Math. Biosci. Eng.* 19.4 (2022), pp. 3402–3426. DOI: 10.3934/mbe.2022157 (cit. on p. C23).

## Author addresses

1. **Siti Nurnabihah Karim**, Department of Mathematical Sciences, Faculty of Science, Universiti Teknologi Malaysia, Malaysia
mailto:sitinurnabihah9@gmail.com

2. **Tau Keong Ang**, Department of Mathematical Sciences, Faculty of Science, Universiti Teknologi Malaysia, Malaysia
mailto:taukeong@utm.my

3. **Hamizah Mohd Safuan**, Department of Mathematics and Statistics, Faculty of Applied Sciences and Technology, Universiti Tun Hussein Onn Malaysia, Malaysia
mailto:hamizahs@uthm.edu.my

4. **Sze Qi Chan**, Southampton Malaysia Business School, University of Southampton Malaysia, Malaysia Smart Manufacturing and Systems Research Group, University of Southampton Malaysia, Malaysia
mailto:s.q.chan@soton.ac.uk